

# Frequency-domain methods for a vibration-fatigue-life estimation - Application to real data

Matjaž Mršnik, Janko Slavič, Miha Boltežar  
Faculty of Mechanical Engineering, University of Ljubljana, Slovenia

February 10, 2016

## Cite as:

Matjaž Mršnik, Janko Slavič and Miha Boltežar  
**Frequency-domain methods for a vibration-fatigue-life estimation - Application to real data.**  
**International Journal of Fatigue, Vol. 47, p. 8-17, 2013.**  
**DOI: 10.1016/j.ijfatigue.2012.07.005**

## Abstract

The characterization of vibration-fatigue strength is one of the key parts of mechanical design. It is closely related to structural dynamics, which is generally studied in the frequency domain, particularly when working with vibratory loads. A fatigue-life estimation in the frequency domain can therefore prove advantageous with respect to a time-domain estimation, especially when taking into consideration the significant performance gains it offers, regarding numerical computations. Several frequency-domain methods for a vibration-fatigue-life estimation have been developed based on numerically simulated signals. This research focuses on a comparison of different frequency-domain methods with respect to real experiments that are typical in structural dynamics and the automotive industry. The methods researched are: Wirsching-Light, the  $\alpha_{0.75}$  method, Gao-Moan, Dirlik, Zhao-Baker, Tovo-Benasciutti and Petrucci-Zuccarello. The experimental comparison researches the resistance to close-modes, to increased background noise, to the influence of spectral width, and multi-vibration-mode influences. Additionally, typical vibration profiles in the automotive industry are also researched. For the experiment an electrodynamic shaker with a vibration controller was used. The reference-life estimation is the rainflow-counting method with the Palmgren-Miner summation rule. It was found that the Tovo-Benasciutti method gives the best estimate for the majority of experiments, the only exception being the typical automotive spectra, for which the enhanced Zhao-Baker method is best suited. This research shows that besides the Dirlik approach, the Tovo-Benasciutti and Zhao-Baker methods should be considered as the preferred methods for fatigue analysis in the frequency domain.

## Nomenclature

$a$	peak amplitude
$a(\cdot)$	best fitting parameters (Wirsching-Light method)
$b(\cdot)$	best fitting parameters (Wirsching-Light method)
$k$	$S$ - $N$ slope coefficient
$C$	$S$ - $N$ curve constant
$d$	eq. root for calc. of fatigue life (Zhao-Baker method)
$\bar{D}$	damage intensity
$\bar{D}_{RFC}$	rainflow damage intensity
$f$	frequency
$f_0$	central frequency
$\Delta f$	mode bandwidth at half-power points
$G_1 - G_3$	Dirlik method parameters
$G_{XX}$	one-sided power spectral density
$H(\omega)$	frequency response function
$H(\omega)$	acceleration to stress frequency-transfer function
$m$	stress range mean
$m_i$	$i$ -th moment of power spectral density
$N$	number of cycles to failure
$p_p(\cdot)$	probability density function of peaks
$p_a(\cdot)$	cycle amplitude probability density function
$Q$	quality factor or Dirlik method parameter
$r$	stress range
$r_e$	Goodman equivalent stress range
$R$	Dirlik method parameter
$R_H(t)$	high-frequency random process
$R_M(t)$	intermediate-frequency random process
$R_L(t)$	low-frequency random process
$s$	stress amplitude
$S_u$	tensile strength
$S_{FF}$	force excitation spectra
$S_{XX}$	power spectral density or displacement response spectra
$T$	fatigue life estimate
$T_{err}$	relative error of fatigue-life estimate
$w$	weighting factor (Zhao-Baker method)
$X$	random process
$x_m$	mean frequency (Dirlik method)
$x_{\max}$	absolute maximum value of stress
$Z$	normalized amplitude
$\alpha$	Weibull distribution parameter
$\alpha_i$	( $\alpha_2$ , spectral width parameters)
$\alpha_{0.75})$	
$\beta$	Weibull distribution parameter
$\gamma$	maximum stress $x_{\max}$ to tensile strength $S_u$ ratio

$\Gamma(\cdot)$	the Euler gamma function
$\delta$	Vanmarcke's bandwith parameter
$\varepsilon$	spectral width parameter
$\nu_0$	expected positive zero-crossing frequency
$\nu_p$	expected peak occurrence frequency
$\rho_{WL}$	empirical correction factor (Wirsching-Light method)
$\rho_{ZB}$	correction factor (Zhao-Baker method)
$\sigma_X^2$	random process variance
$\chi_k$	$k$ -th moment of cycle amplitude probability density
$\Phi(\cdot)$	standard normal cumulative distribution function
$\Psi(\cdot)$	approximation function (Petrucci-Zuccarello method)
$\Psi_1 - \Psi_4$	approx. function coeff. (Petrucci-Zuccarello method)
<b>a</b>	forced vibration acceleration profile
[C]	damping matrix
{f}	forced vibration vector
<b>H<sub>as</sub></b>	frequency-response function matrix (acc. to stress)
[K]	stiffnes matrix
[M]	mass matrix
<b>s</b>	normal stress tensor
{x}	degree-of-freedom vector
AL	the $\alpha_{0.75}$ method
DK	Dirlik method
GM	Gao-Moan method
NB	narrow-band method
PZ	Petrucci-Zuccarello method
TB1	Tovo-Benasciutti method
TB2	improved Tovo-Benasciutti method
WL	Wirsching-Light method
ZB1	Zhao-Baker method
ZB2	improved Zhao-Baker method
AM	typical automotive spectra
BN	increased background noise spectra
CM	close-modes spectra
MM	multi-mode spectra
SW	spectral width spectra

## 1 Introduction

Fatigue is a common cause of failure in mechanical structures and components subjected to time-variable loadings [1]. It is critical that fast and effective tools are available to estimate the fatigue life during the design process. Frequency-domain methods for fatigue assessment aim to speed up the calculations substantially, as they define the loading process in the frequency domain.

A well-established practice of fatigue assessment consists of a determination of the loading history, the identification of damaging cycles [2] and an evaluation

of the total fatigue damage by aggregating the damage contributions [3, 4] of the respective damaging cycles [5].

In the time domain the identification of cycles in an irregular loading history is accomplished by means of a cycle-counting method, usually employing the rainflow algorithm that was introduced by Matsuishi and Endo [2]. The accumulation of damage is then carried out according to the hypothesis of linear damage accumulation, which was independently presented by Palmgren [3] and Miner [4]. The combination of rainflow counting and Palmgren-Miner has been tried and tested thoroughly and is generally accepted as one of the best time-domain methods for a fatigue-life estimation [1, 6, 7, 8, 9].

In reality, structures such as a car on a rough road or a wind turbine are exposed to random loads (*e.g.*, road surface, wind speed). Such random loads can be viewed as the realization of a random Gaussian process that can be described in the frequency domain by a power spectral density [5], representing the spread of the mean square amplitude over a frequency range [10]. Operating with a power spectral density proves especially beneficial when working with complicated finite-element models where the calculation of the frequency response is much faster than a transient dynamic analysis in the time domain [6].

Long time histories can be simulated as samples of a random process, defined in the frequency domain. However, this approach is not an ideal design tool [11].

A different approach is the development of frequency-domain methods for a fatigue assessment that offer a direct connection between the power spectral density and the damage intensity or the cycle distribution of loading. As most authors consider the rainflow method to be the most accurate, the frequency-domain methods try to obtain a cycle distribution according to rainflow counting in the time domain [7, 12, 13].

The methods described here are concerned with the stationary Gaussian process. It is further divided into narrow-band and wide-band processes, of which the narrow-band allows for a straightforward derivation of the cycle distribution, as pointed out by Lutes and Sarkani [11]. For a wide-band process the relation of the peak distribution and cycle amplitudes is much more complex. Several empirical solutions (*e.g.*, Dirlit [12] and Zhao-Baker [7]) have been proposed, but only very few completely theoretical solutions (*e.g.*, Bishop [14]). The theoretical solution presented by Bishop is based on the Markov process theory and is computationally intensive. However, it shows little improvement in accuracy over Dirlit, which is usually the preferred method [6].

Frequency-domain methods are used in different fields, such as structural health monitoring [15], the FEM environment [16], multi-axial fatigue [17] and a non-normal process fatigue evaluation with the use of a correction factor [18].

Since the introduction of Dirlit and Bishop several comparison studies have been made [19, 20, 13, 5, 21]. These comparison studies show that the Dirlit method performs better than most of the other methods.

In 2004 Benasciutti and Tovo [22] compared a group of frequency-domain methods, *i.e.*, Wirsching-Light [23], Zhao-Baker [7], Dirlit [12], the empirical  $\alpha_{0.75}$  [22], and Tovo-Benasciutti [8, 13], and found that the Tovo-Benasciutti method matches the accuracy of the Dirlit method in terms of numerically

simulated power spectral densities. A thorough study of fatigue evaluation for a multi-axial random loading was made by Lagoda et. al. [24]. Experiment showed a good agreement with the fatigue-life estimate of the Wirsching-Light method. Braccesi et. al. [25] developed the Percentage Error Index (IEP) by which they compared the Dirlit, Zhao-Baker, Fu-Cebon [26], Sakai-Okamura [27] and Bendat [28] methods on bi-modal triangular spectra. Results produced by the Dirlit method were again among the best and most consistent. Special case is a new method by Gao and Moan [21], which is based on similar principles as bi-modal methods, but can be generalized for a broad-band spectra.

A subdomain group of frequency-domain methods, such as Sakai-Okamura [27] and Fu-Cebon [26], are aimed at evaluating bi-modal processes which can often represent two modal shapes of a structure response spectra. Recent work has been done in this field by Low [29], demonstrating the exceptional accuracy that can be attained using the bi-modal formulation. However, the focus of this paper is on frequency-domain methods that can be used blindly across different broad-band random processes and thus bi-modal methods are not explored in detail.

In this research, a theoretical and experimental comparison of several frequency-domain methods is given. Some of those methods are for the first time compared side-by-side. Existing studies already deal with experimental validation of results, namely Lagoda et al. [24, 30] and Kim et al. [31]. In this research the focus is on performance of selected frequency-domain-methods with different groups of spectra with the aim of finding a most accurate frequency-domain method(s) for blind use on different broad-band processes.

Besides localized effects, the stress distribution of a real structure significantly relates to the structural dynamics [32]. The frequency-domain methods are researched with regards to the structural dynamics properties: close-modes, increased background noise, number of modes and spectral width. Typical vibration profiles used in automotive accelerated tests are also researched. For this purpose, different vibration profiles are devised, which are varied according to one of the listed dynamic properties.

This research is organized as follows: Section 2 gives the theoretical background of different frequency-domain methods. Section 3 briefly presents some selected frequency-domain methods for a fatigue-life evaluation and cycle-distribution estimation. In Section 4 the experimental set-up is explained, followed by a discussion of the results in Section 5 and, finally, the conclusions are given in Section 6.

## 2 Theoretical background

To facilitate an understanding of frequency-domain methods and their definitions, a brief introduction to the stochastic process theory will be presented first. For a deeper understanding and an elaborate derivation the reader is referred to the reference works of Shin and Hammond [10] and Newland [33]. The basics of the modal analysis that can be used to determine the stress function

at different material points of the vibrating structure are covered next. Finally, a general approach to specifying the fatigue strength in the frequency domain is presented.

## 2.1 Properties of random processes

In the frequency domain the random loading of a random process  $X$  is defined by the power spectral density  $S_{XX}(f)$ , with  $f$  denoting the frequency. It is customary to use a one-sided power spectral density  $G_{XX}(f)$ , defined on the positive half-axis only. The statistical properties of a stationary process can be described by the moments of the power spectral density. The general form for the  $i$ -th spectral moment  $m_i$  is given by:

$$m_i = \int_0^\infty f^i G_{XX}(f) df. \quad (1)$$

For a fatigue analysis the moments up to  $m_4$  are normally used. The even moments represent the variance  $\sigma_X^2$  of the random process  $X$  and its derivatives:

$$\sigma_X^2 = m_0 \quad \sigma_{\dot{X}}^2 = m_2 \quad (2)$$

The spread of the process or the spectral width is estimated using the parameter  $\alpha_i$ , which has the general form:

$$\alpha_i = \frac{m_i}{\sqrt{m_0 m_{2i}}} \quad (3)$$

The most commonly used  $\alpha_2$  is the negative of the correlation between the process and its second derivative, as described by Tovo [8]. It takes values from 0 to 1. The higher the value, the narrower is the process in the frequency domain and vice-versa.

Another frequently used spectral parameter is Vanmarcke's parameter  $\delta$  [34]:

$$\delta = \sqrt{1 - \alpha_1^2} \quad (4)$$

The expected peak occurrence frequency  $\nu_p$  and the expected positive zero-crossing rate  $\nu_0$  are defined as:

$$\nu_p = \sqrt{\frac{m_4}{m_2}} \quad \nu_0 = \sqrt{\frac{m_2}{m_0}} \quad (5)$$

They are imperative for determining the fatigue-life intensity. The analytical derivation of both was described by Newland [33].

The foundations for a frequency-domain approximation of a cycle distribution were set by Rice [35], who managed to analytically define the probability density function of the peaks  $p_p(a)$  based on the power spectral density:

$$p_p(a) = \frac{\sqrt{1 - \alpha_2^2}}{\sqrt{2\pi}\sigma_X} e^{-\frac{a^2}{2\sigma_X^2(1-\alpha_2^2)}} + \frac{\alpha_2 a}{\sigma_X^2} e^{-\frac{a^2}{2\sigma_X^2}} \Phi\left(\frac{\alpha_2 a}{\sigma_X \sqrt{1 - \alpha_2^2}}\right) \quad (6)$$

where  $a$  is the peak amplitude and  $\sigma_X$  and  $\alpha_2$  are defined with Equations (2) and (3), respectively.  $\Phi(z)$  is the standard normal cumulative distribution function:

$$\Phi(z) = \frac{1}{\sqrt{2\pi}} \int_{-\infty}^z e^{-\frac{t^2}{2}} dt \quad (7)$$

## 2.2 Structural dynamics and modal analysis

The objective of the modal analysis is to establish a mathematical model of the structure. The structural dynamics and the response can already be characterized during the design stage, usually with the help of FEM methods [16, 32, 36]. The linear structural dynamics is described in the frequency domain, which is why the frequency-domain methods for fatigue analysis are of great interest. Recent research [17] even suggests it is possible to evaluate more complicated multi-axial loadings in the same manner. So as not to lose focus, here only the basics are given and the interested reader is advised to read references [37, 36].

Complex structures can be viewed as linear, multi-degree-of-freedom systems that are described by a system of second-order differential equations [37]:

$$[\mathbf{M}] \{ \ddot{\mathbf{x}} \} + [\mathbf{C}] \{ \dot{\mathbf{x}} \} + [\mathbf{K}] \{ \mathbf{x} \} = \{ \mathbf{f} \} \quad (8)$$

where  $[\mathbf{M}]$  is the mass matrix,  $[\mathbf{C}]$  is the damping matrix,  $[\mathbf{K}]$  is the stiffness matrix,  $\{ \mathbf{x} \}$  is the vector of degrees of freedom and  $\{ \mathbf{f} \}$  is the excitation force vector. Furthermore, through modal analysis the transfer functions from one point on the structure to the other can be deduced, mathematically or by experiment.

For a selected geometrical location on the structure the displacement response spectra  $S_{XX}(\omega)$  can be obtained by knowing the frequency-response function  $H(\omega)$  (phase information is truncated with PSD, thus  $|H(\omega)|^2$ ) and the force excitation spectra  $S_{FF}(\omega)$  [37]:

$$S_{XX}(\omega) = |H(\omega)|^2 S_{FF}(\omega) \quad (9)$$

The response characteristics other than the displacements (*e.g.*, stress, acceleration) can also be expressed. As mechanical structures are usually exposed to a known acceleration profile, for a fatigue analysis the frequency-transfer function  $H_{as}(\omega)$  from the acceleration  $a$  to the material stress  $s$  is of special interest.

For multi-degree-of-freedom systems the response is dependent on multiple inputs and Equation (9) is rewritten in the matrix form as:

$$\mathbf{s} = \mathbf{H}_{\mathbf{as}} \mathbf{a} \quad (10)$$

where  $\mathbf{s}$  is the normal stress tensor in the frequency domain,  $\mathbf{a}$  is the forced vibration acceleration profile and  $\mathbf{H}_{\mathbf{as}}$  is the frequency-response function matrix.

### 2.3 Fatigue-life estimation

A possible scenario in fatigue analysis is to numerically simulate the operating time until failure for a structural member with a given critical stress function in the frequency domain at selected node(s) (10). Instead of the time-until-failure criteria, this research focuses on the damage intensity  $\bar{D}$ , see Benasciutti and Tovo [13]. The damage intensity estimates the damage per unit of time. It is defined with:

$$\bar{D} = \nu_p C^{-1} \int_0^\infty s^k p_a(s) ds, \quad (11)$$

where  $\nu_p$  is the expected peak occurrence frequency, given by Equation (5),  $C$  and  $k$  are material parameters and  $p_a(s)$  is the cycle amplitude probability density function. The function  $p_a(s)$  is the unknown and a key factor considered by frequency-domain methods for fatigue analyses.

The evaluation of frequency-domain methods is carried out by a comparison of the fatigue-life estimate  $T$  in seconds, which is obtained from the damage intensity  $\bar{D}$ :

$$T = \frac{1}{\bar{D}} \quad (12)$$

## 3 Frequency-domain methods

Typical methods for fatigue analyses in the frequency domain designed to deal with Gaussian random loadings are discussed in this section. While the narrow-band (NB) approximation is only appropriate for narrow-band processes, others are also appropriate for wide-band loading processes. These are the Wirsching-Light method (WL) [23], the  $\alpha_{0.75}$  method (AL) [22], the Gao-Moan method (GM) [21], the Dirlik method (DK) [12], both Zhao-Baker methods (ZB1 and ZB2) [7], the Tovo-Benasciutti methods (TB1 and TB2) [8, 13] and the Petrucci-Zuccarello method (PZ) [9]. The  $\alpha_{0.75}$  method and the Wirsching-Light method differ from the others in the way that they provide the correction factor to correct the narrow-band approximation for wide-band processes.

### 3.1 Narrow-band approximation

For a narrow-band process it is reasonable to assume that every peak is coincident with a cycle and that, consequently, the cycle amplitudes are Rayleigh-distributed. The narrow-band expression was originally presented by Miles in 1956 [38] and is here defined for stress amplitudes:

$$\bar{D}^{\text{NB}} = \nu_0 C^{-1} (\sqrt{2 m_0})^k \Gamma \left( 1 + \frac{k}{2} \right) \quad (13)$$

where  $\nu_0$  is the expected positive zero-crossings intensity, which is very close to the peak intensity  $\nu_p$  for a narrow-band process,  $C$  and  $k$  are material fatigue parameters,  $m_0$  is the 0-th spectral moment,  $\alpha_2$  is determined with (3) and  $\Gamma(\cdot)$  is the Euler gamma function, which is defined as:

$$\Gamma(z) = \int_0^\infty t^{z-1} e^{-t} dt \quad (14)$$

### 3.2 Wirsching-Light method

Wirsching and Light [23] in 1980 used an additional spectral width parameter  $\alpha_2$  to correct the narrow-band approximation with the empirical factor  $\rho_{\text{WL}}$ :

$$\bar{D}^{\text{WL}} = \rho_{\text{WL}} \bar{D}^{\text{NB}} \quad (15)$$

where  $\bar{D}^{\text{NB}}$  is the narrow-band approximation obtained with Equation (13) and  $\rho_{\text{WL}}$  is defined as:

$$\rho_{\text{WL}} = a(k) + [1 - a(k)] (1 - \varepsilon)^{b(k)} \quad (16)$$

with the spectral width parameter  $\varepsilon$  being:

$$\varepsilon = \sqrt{1 - \alpha_2^2} \quad (17)$$

and the best fitting parameters  $a(\cdot)$  and  $b(\cdot)$  dependent on the *S-N* slope  $k$ :

$$a(k) = 0.926 - 0.033 k \quad b(k) = 1.587 k - 2.323 \quad (18)$$

where the authors used the *S-N* slope  $k$  values of 3, 4, 5 and 6 for the simulations.

### 3.3 $\alpha_{0.75}$ method

The second correction method, named  $\alpha_{0.75}$ , is simple yet agrees fairly well with the data from the numerical simulation according to Benasciutti and Tovo, who also propose this method [22]. It is based on the spectral parameter  $\alpha_{0.75}$  and is given with:

$$\overline{D}^{\text{AL}} = \alpha_{0.75}^2 \overline{D}^{\text{NB}} \quad (19)$$

where  $\overline{D}^{\text{NB}}$  is the narrow-band approximation (13) and  $\alpha_{0.75}$  is defined with (3).

### 3.4 Gao-Moan method

Recently, a trimodal method was presented by Gao and Moan [21] along with a generalized variant that can be applied to other (wide-band) types of processes. The fatigue-damage intensity  $\overline{D}^{GM}$  is the sum of the high-frequency process  $R_H(t)$ , the intermediate-frequency process  $R_M(t)$  and the low-frequency process  $R_L(t)$  contributions, each are being narrow-banded and having a Rayleigh-distributed amplitude with the respective variances equal to  $\sigma_H$ ,  $\sigma_M$ ,  $\sigma_L$ :

$$\overline{D}^{GM} = \overline{D}_P + \overline{D}_Q + \overline{D}_H \quad (20)$$

where  $R_H(t)$  is treated as a narrow-band process and  $\overline{D}_P$  and  $\overline{D}_Q$  are damage intensities due to the processes  $R_P(t)$  and  $R_Q(t)$ , respectively:

$$\begin{aligned} R_P(t) &= R_H(t) + R_M(t) \\ R_Q(t) &= R_H(t) + R_M(t) + R_L(t) \end{aligned} \quad (21)$$

The damage component  $\overline{D}_H$  is determined using (13), where  $\nu_{0H}$  is given by (5). Equation (11) is used for  $\overline{D}_P$  and  $\overline{D}_Q$ , where the expected zero-crossing frequencies are used instead of the peak frequencies and are calculated with:

$$\nu_{0P} = \sqrt{m_{2H} \delta_H^2 + m_{2M}} \frac{\sigma_M}{(\sigma_H^2 + \sigma_M^2)} \quad (22)$$

$$\begin{aligned} \nu_{0Q} &= \sqrt{m_{2H} \delta_H^2 + m_{2M} \delta_M^2 + m_{2L}} \\ &\times \left[ \frac{2 \sigma_L \sqrt{\sigma_H^2 + \sigma_M^2 + \sigma_L^2} - \pi \sigma_H \sigma_M}{2 \left( \sqrt{\sigma_H^2 + \sigma_M^2 + \sigma_L^2} \right)^3} \right. \\ &\left. + \frac{2 \sigma_H \sigma_M \arctan \frac{\sigma_H \sigma_M}{\sigma_L \sqrt{\sigma_H^2 + \sigma_M^2 + \sigma_L^2}}}{2 \left( \sqrt{\sigma_H^2 + \sigma_M^2 + \sigma_L^2} \right)^3} \right] \end{aligned} \quad (23)$$

where  $\delta_H$  and  $\delta_M$  are Vanmarcke's parameters from Equation (4), calculated for the processes  $R_H(t)$  and  $R_M(t)$ , respectively. The probability density functions for the sum of two or more random variables, also needed for calculating (11), are determined by means of the convolution integral:

$$p_{a,HM} = \int_0^\infty p_{a,H}(s) p_{a,M}(t-s) ds \quad (24)$$

$$p_{a,HML} = \int_0^\infty p_{a,HM}(s) p_{a,L}(t-s) ds \quad (25)$$

where  $p_{a,H}$ ,  $p_{a,M}$  and  $p_{a,L}$  are the cycle-amplitude probability densities of the respective narrow-band processes. Hermite integration was used by Gao and Moan to calculate the distribution of the sum of the multiple Rayleigh random variables [21].

The trimodal approach is generalized to a general wide-band process by splitting the power spectral density into three parts, according to the chosen criteria. The authors recommend splitting into three parts with equal variance, with each part then being treated as one of the three modes. This same approach is used in this paper, referenced with GM. Additionally, the accuracy of the Gao-Moan method could be improved by using a higher order, multi-modal formulation of the method, such as a four- or five-modal formulation [21].

### 3.5 Dirlik method

The Dirlik method [12], devised in 1985, approximates the cycle-amplitude distribution by using a combination of one exponential and two Rayleigh probability densities. It is based on numerical simulations of the time histories for two different groups of spectra. This method has long been considered to be one of the best and has already been subject to modifications, *e.g.*, for the inclusion of the temperature effect, by Zalaznik and Nagode [39]. The rainflow-cycle amplitude probability density estimate is given by:

$$p_a(s) = \frac{1}{\sqrt{m_0}} \left[ \frac{G_1}{Q} e^{\frac{-Z}{Q}} + \frac{G_2 Z}{R^2} e^{\frac{-Z^2}{2R^2}} + G_3 Z e^{\frac{-Z^2}{2}} \right] \quad (26)$$

where  $Z$  is the normalized amplitude and  $x_m$  is the mean frequency, as defined by the author of the method [12]:

$$Z = \frac{s}{\sqrt{m_0}} \quad x_m = \frac{m_1}{m_0} \left( \frac{m_2}{m_4} \right)^{\frac{1}{2}} \quad (27)$$

and the parameters  $G_1$  to  $G_3$ ,  $R$  and  $Q$  are defined as:

$$\begin{aligned} G_1 &= \frac{2(x_m - \alpha_2^2)}{1 + \alpha_2^2} & G_2 &= \frac{1 - \alpha_2 - G_1 + G_1^2}{1 - R} \\ G_3 &= 1 - G_1 - G_2 & R &= \frac{\alpha_2 - x_m - G_1^2}{1 - \alpha_2 - G_1 + G_1^2} \\ Q &= \frac{1,25(\alpha_2 - G_3 - G_2 R)}{G_1} \end{aligned} \quad (28)$$

while  $\alpha_2$  has already been defined with Equation (3). The closed-form expression for the fatigue-life intensity has been derived in the form:

$$\begin{aligned} \bar{D}^{\text{DK}} &= C^{-1} \nu_p m_0^{\frac{k}{2}} [G_1 Q^k \Gamma(1+k) \\ &\quad + (\sqrt{2})^k \Gamma(1 + \frac{k}{2}) (G_2 |R|^k + G_3)] \end{aligned} \quad (29)$$

### 3.6 Zhao-Baker method

This method was developed by Zhao and Baker in 1992 [7]. It combines theoretical assumptions and simulation results to give an expression for the cycle distribution as a linear combination of the Weibull and Rayleigh probability density function:

$$p_a(Z) = \underbrace{w \alpha \beta Z^{\beta-1} e^{-\alpha Z^\beta}}_{\text{Weibull}} + \underbrace{(1-w) Z e^{-\frac{Z^2}{2}}}_{\text{Rayleigh}} \quad (30)$$

where  $Z$  is the normalized amplitude from Equations (27) and  $w$  is the weighting factor defined by:

$$w = \frac{1 - \alpha_2}{1 - \sqrt{\frac{2}{\pi}} \Gamma\left(1 + \frac{1}{\beta}\right) \alpha^{-1/\beta}} \quad (31)$$

and  $\alpha$  and  $\beta$  are the Weibull parameters:

$$\alpha = 8 - 7 \alpha_2 \quad (32)$$

$$\beta = \begin{cases} 1.1; & \alpha_2 < 0, 9 \\ 1.1 + 9(\alpha_2 - 0, 9); & \alpha_2 \geq 0.9 \end{cases} \quad (33)$$

According to Equation (30) the Rayleigh part corresponds mainly to the large cycle amplitudes and the Weibull part to small amplitudes when looking at the cycle-amplitude distribution.

For the spectral width parameter  $\alpha_2 < 0.13$  the expression for the weighting factor  $w$  gives the incorrect results  $w > 1$  and therefore the Zhao-Baker method is not suitable for those cases [22]. Also, because the simulations were only concerned with the values of  $2 \leq k \leq 6$  the model should be re-evaluated to reach a good agreement for higher values of the  $S$ - $N$  slope  $k$  [7].

For small values of the  $S$ - $N$  slope  $k$  ( $k = 3$ ) the rainflow damage is more closely related to  $\alpha_{0.75}$  than  $\alpha_2$ . Zhao and Baker offered an enhanced method of their calculation (ZB2) where  $\alpha$  is calculated as:

$$\alpha = d^{-\beta} \quad (34)$$

with  $d$  calculated as a root of:

$$\begin{aligned} \Gamma\left(1 + \frac{3}{\beta}\right) (1 - \alpha_2) d^3 + 3 \Gamma\left(1 + \frac{1}{\beta}\right) (\rho_{\text{ZB}} \alpha_2 - 1) d + \\ + 3 \sqrt{\frac{\pi}{2}} \alpha_2 (1 - \rho_{\text{ZB}}) = 0 \end{aligned} \quad (35)$$

and the correction factor  $\rho_{\text{ZB}}$  at  $k = 3$  is determined by:

$$\rho_{\text{ZB}}|_{k=3} = \begin{cases} -0.4154 + 1.392 \alpha_{0.75}; & \alpha_{0.75} \geq 0.5 \\ 0.28; & \alpha_{0.75} < 0.5 \end{cases} \quad (36)$$

A closed-form expression for directly calculating the fatigue-damage intensity is defined with [22]:

$$\overline{D}^{\text{ZB1/ZB2}} = \frac{\nu_p}{C} m_0^{k/2} \left[ w \alpha^{-\frac{k}{\beta}} \Gamma\left(1 + \frac{k}{\beta}\right) + (1 - w) 2^{k/2} \Gamma\left(1 + \frac{k}{2}\right) \right] \quad (37)$$

where the use of the ordinary approach is denoted with ZB1 and the use of the enhanced method with ZB2.

### 3.7 Tovo-Benasciutti method

In 2002, Benasciutti and Tovo [8, 13] first proposed an approach where the fatigue life is calculated as a linear combination of the upper and lower fatigue-damage intensity limits. The final expression for the estimated fatigue-damage intensity is:

$$\overline{D}^{\text{TB}} = [b + (1 - b) \alpha_2^{k-1}] \alpha_2 \overline{D}^{\text{NB}} \quad (38)$$

where  $b$  is unknown and is approximated with numerical simulation data. The narrow-band damage intensity  $\bar{D}^{\text{NB}}$  is defined with Equation (13), where the zero-crossing intensity  $\nu_0$  is replaced with the peak intensity  $\nu_p$  for wide-band processes. Similarly, the rainflow amplitudes' probability density  $p_a(s)$  estimate can also be written in the form of a linear combination of two probability densities [22].

Two different equations are suggested for determining the factor  $b$  in order to substitute into Equation (38), both were proposed by Benasciutti and Tovo [8, 13]:

$$b_{\text{app}}^{\text{TB1}} = \min \left\{ \frac{\alpha_1 - \alpha_2}{1 - \alpha_1}, 1 \right\} \quad (39)$$

$$b_{\text{app}}^{\text{TB2}} = \frac{(\alpha_1 - \alpha_2) [1.112 (1 + \alpha_1 \alpha_2 - (\alpha_1 + \alpha_2)) e^{2.11 \alpha_2} + (\alpha_1 - \alpha_2)]}{(\alpha_2 - 1)^2} \quad (40)$$

where using the  $b_{\text{app}}^{\text{TB1}}$  from Equation (39) will be referenced with TB1 and using  $b_{\text{app}}^{\text{TB2}}$  from Equation (40) with TB2.

### 3.8 Petrucci-Zuccarello method

This method was proposed in 2004 by Petrucci and Zuccarello [9] who sought a connection between the moments of the probability density of the equivalent Goodman stress and the parameters  $\alpha_1$ ,  $\alpha_2$ ,  $k$  and  $\gamma$ , the last of these being the ratio:

$$\gamma = \frac{x_{\max}}{S_u} \quad (41)$$

where  $x_{\max}$  is the absolute maximum value of the stress process and  $S_u$  is the material tensile strength.

As already mentioned, the Petrucci-Zuccarello method implicitly predicts equivalent stress ranges by calculating the Goodman equivalent stress range [40]:

$$r_e = \frac{r}{1 - \frac{m}{S_u}} \quad (42)$$

where  $r$  is the original stress range,  $m$  is the range mean and  $S_u$  is the tensile strength. The expression for calculating the damage-intensity estimate is:

$$\bar{D}^{\text{PZ}} = C^{-1} \nu_p \sqrt{m_0^k} e^{\Psi(\alpha_1, \alpha_2, b, \gamma)} \quad (43)$$

where  $\nu_p$  is defined with (5) and the spectral moment  $m_0$  with (1). The approximation function  $\Psi(\cdot)$  [9]:

$$\begin{aligned}\Psi(\alpha_1, \alpha_2, k, \gamma) = & \frac{(\Psi_2 - \Psi_1)}{6} (b - 3) + \Psi_1 + \left[ \frac{2}{9} (\Psi_4 - \Psi_3) \right. \\ & \left. - (\Psi_2 + \Psi_1) (k - 3) + \frac{4}{3} (\Psi_3 - \Psi_1) \right] (\gamma - 0, 15)\end{aligned}\quad (44)$$

depends on the material parameter  $k$ , the ratio  $\gamma$  and the coefficients  $\Psi_1$  to  $\Psi_4$  given as polynomials:

$$\begin{aligned}\Psi_1 = & -1,994 - 9,381 \alpha_2 + 18,349 \alpha_1 \\ & + 15,261 \alpha_1 \alpha_2 - 1,483 \alpha_2^2 - 15,402 \alpha_1^2 \\ \Psi_2 = & 8,229 - 26,510 \alpha_2 + 21,522 \alpha_1 \\ & + 27,748 \alpha_1 \alpha_2 + 4,338 \alpha_2^2 - 20,026 \alpha_1^2 \\ \Psi_3 = & -0,946 - 8,025 \alpha_2 + 15,692 \alpha_1 \\ & + 11,867 \alpha_1 \alpha_2 + 0,382 \alpha_2^2 - 13,198 \alpha_1^2 \\ \Psi_4 = & 8,780 - 26,058 \alpha_2 + 21,628 \alpha_1 \\ & + 26,487 \alpha_1 \alpha_2 + 5,379 \alpha_2^2 - 19,967 \alpha_1^2\end{aligned}\quad (45)$$

with  $\alpha_1$  and  $\alpha_2$  taken from Equation (3).

## 4 Experiment

In real life dynamical structures exposed to vibrations respond according to their natural dynamics, and to avoid real-life (in application) experiments, accelerated tests are used. The load during accelerated vibration tests is based on real-life vibration loads, but these tests are usually accelerated with higher vibration amplitudes. The accelerated vibration tests are usually made by using electro-dynamical shakers, where a controlled excitation profile in the frequency domain is used. According to Equation (10) the excitation profile is controlled at a selected point of the structure and this results in a stress tensor frequency profile at all the other points. The transfer function from the excitation to the response differs for each material point; so as not to focus on the structure, the excitation acceleration profile is considered as the stress profile and analyzed from the point of the damage estimation ( $1 \text{ m/s}^2$  is considered  $1 \text{ MPa}$ )<sup>1</sup>. The response profile was simulated on a real electro-dynamical shaker and controlled with an industry-standard vibration controller. The proposed spectra, arranged into groups (multi-mode, spectral width, *etc.*), were devised by the authors based on experience in the field of structural dynamics. The real signal was

---

<sup>1</sup>In a real damage estimation the transfer functions of two material points are required and the damage estimation of these points is straightforward with respect to Equation (10).

then actually measured, by means of experiment, on an electro-dynamic shaker, controlled according to the aforementioned spectra. By this procedure one gains insight into frequency-domain methods performance on spectra exhibiting certain structural dynamics phenomena, while avoiding the cumbersome procedure of dealing with a real structure and controlling its response to achieve the same goal.

#### 4.1 Experimental set-up

The test site consisted of a personal computer for control and data acquisition, an acceleration sensor and electrodynamic shaker equipment, see Figures 1 and 2.

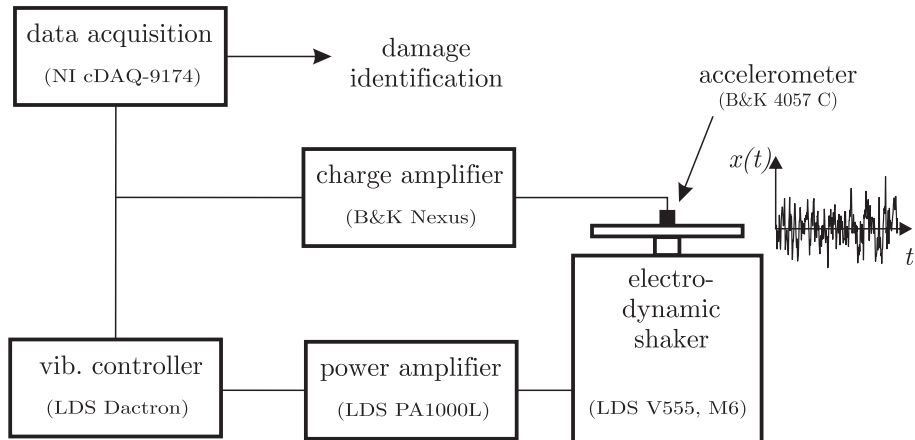


Figure 1: Experiment schematics

Professional hardware and software with a control loop were used to generate the excitation according to a given power spectral density in the range from 10 to 1000 Hz. At the same time, the measured signal was also discretized with a DAQ module and saved for later analysis.

The duration of one measurement was 5 minutes. The sampling frequency was 10000 Hz. The root-mean-square (RMS) value of every random process run on the shaker was 20 MPa.

#### 4.2 Simulated spectra

A number of different power spectral densities were defined in the industry-common frequency-range interval [10 Hz, 1000 Hz]. They are separated into five groups: multi-mode (MM), increased background noise (BN), spectral width (SW), close-modes (CM) and typical automotive spectra (AM).

The quality factor  $Q$  (not to be confused with the Dirlik estimation parameter), also known as the amplification factor [37], is typically used in structural

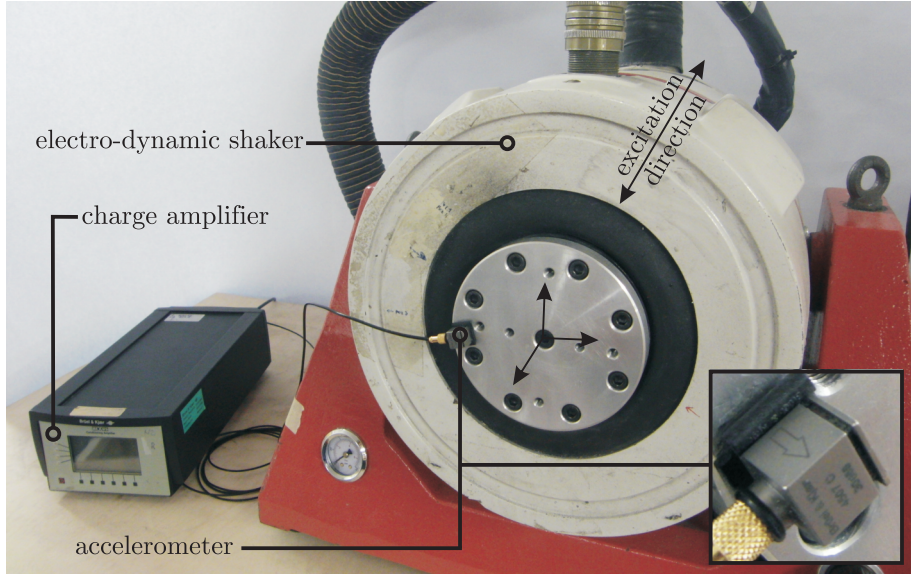


Figure 2: The LDS V555 electro-dynamic shaker with the B&K accelerometer mounted on the vibrating plate and the B&K Nexus charge-conditioning amplifier.

dynamics for a quantitative characterization of the spectral peaks. It conveys information about the sharpness of the resonance or damping, since  $Q = 1/(2\zeta)$  with  $\zeta$  being the damping ratio. The value of  $Q$  was determined based on [37]:

$$Q = \frac{f_0}{\Delta f} \quad (46)$$

where  $f_0$  is the central frequency of the mode and  $\Delta f = f_2 - f_1$  is the mode bandwidth at half-power points, *i.e.*, the frequencies  $f_1$  and  $f_2$ , corresponding to half of the peak amplitude in the frequency domain.

The multi-mode spectra are designed to research the influence of multiple modal frequencies on the fatigue analysis. Initially, there is only one dominant mode, and with each subsequent experiment one additional mode is added (up to a maximum four). This is accomplished by superimposing the modal peaks, as shown in Figure 3. The modes are positioned at the central frequencies  $f_c$  of 200, 400, 600 and 750 Hz with amplitudes of 650 MPa<sup>2</sup>/Hz.

The increased background noise group was selected to research the effect of the background noise on the estimation accuracy in the frequency domain. For this group two modes are always the same: the left mode (see Figure 4) has a quality factor  $Q$  of 5.00 with a central frequency  $f_c = 150$  Hz and the right mode  $Q = 17.96$  with  $f_c = 600$  Hz. In each new experiment, the amplitude of the background noise was increased by 20 MPa<sup>2</sup>/Hz until the smaller peak is

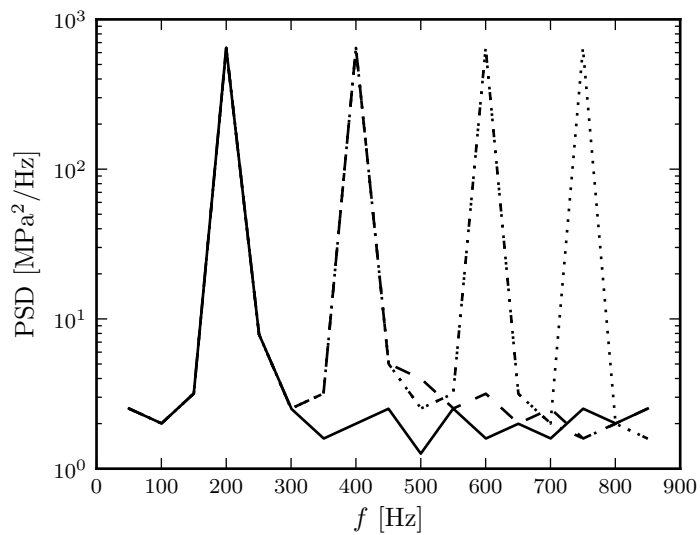


Figure 3: Multi-mode spectra

hidden completely, see Figure 4.

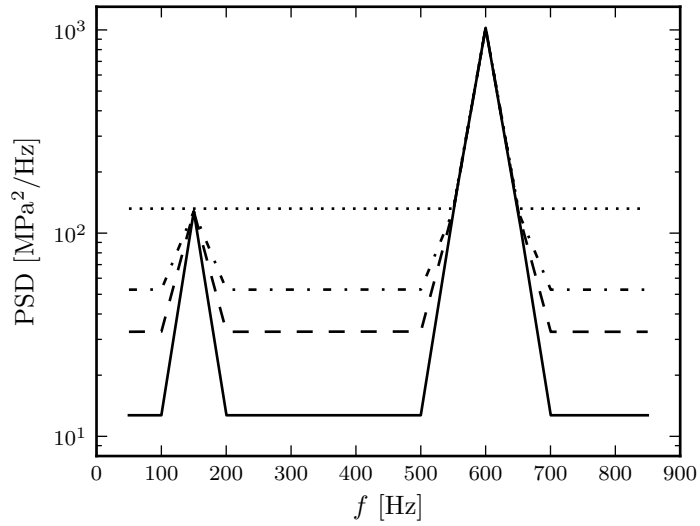


Figure 4: Increased background noise

The spectral width group tested how the spectral width affects the accuracy

of the different spectral methods. In each new experiment the spectral width was broader, as shown in Figure 5. The initial mode with a central frequency of  $f_c = 430$  Hz and factor  $Q = 8.96$  expands by 50 Hz in each direction during each concurrent experiment (up to 450 Hz wide).

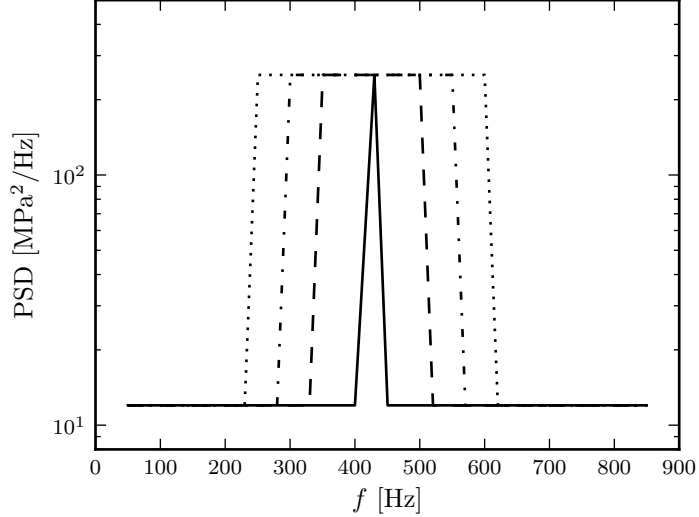


Figure 5: Spectral width group of spectra

The close-modes spectra were used to determine the effect of the close modes on the fatigue-life estimation. In each iteration the peaks with a quality factor of  $Q$  equal to 6.00 and 24.00 and central frequencies  $f_c$  of 150 and 700 Hz, respectively, were 100 Hz closer, as demonstrated in Figure 6.

In accelerated vibration tests, the structure is fixed to the electro-dynamical shaker and excited with a given profile. Because the structural response natural modes discussed above are developed for the frequency region without natural dynamics, the excitation profile is linearly translated to the fatigue loads. Therefore, we investigated three realistic industry spectra that are typical for the automotive industry, shown in Figure 7.

The ranges of the spectral-width parameter  $\alpha_2$  for each group are given in Table 2.

Table 2: Ranges of  $\alpha_2$  parameter for each test group.

	MM	BN	SW	CM	AM
$\alpha_2$	0.49—0.80	0.81—0.92	0.80—0.93	0.73—0.87	0.40—0.48

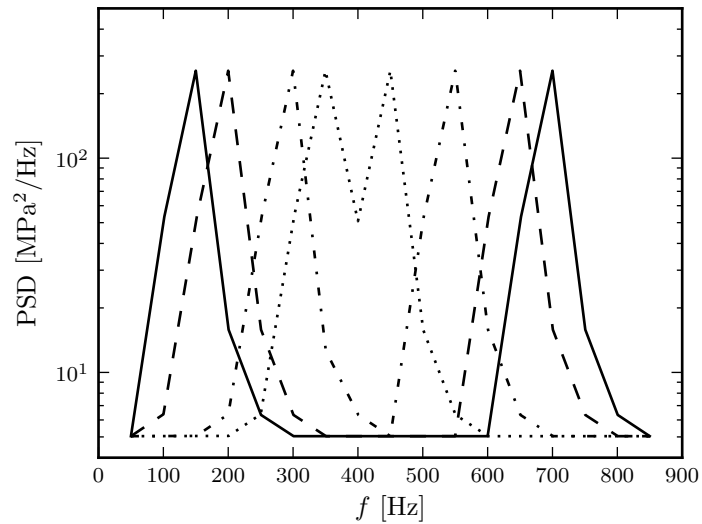


Figure 6: Close-modes spectra

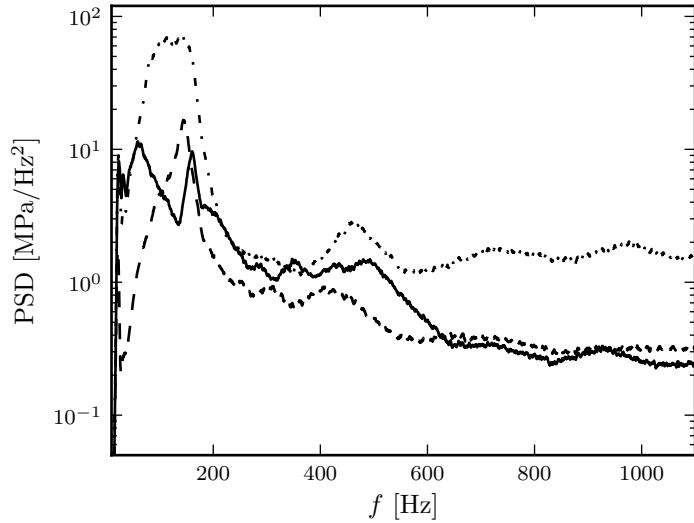


Figure 7: Typical automotive spectra

### 4.3 Results

The fatigue-life estimates for the frequency-domain methods were compared to the life estimate in the time domain using a combination of the rainflow count and the Palmgren-Miner hypothesis,  $T_{RFC}$ , which in this study is assumed to be an exact reference value. The relative error is calculated using:

$$T_{\text{err}} = \frac{T^{\text{XX}} - T_{\text{RFC}}}{T_{\text{RFC}}} \quad (47)$$

where  $T^{\text{XX}}$  is a life estimate, as calculated using one of the frequency-domain methods. Because of the significant impact the  $S-N$  slope  $k$  has on the accuracy of the fatigue-life estimation, three different material parameters, presented by Petrucci and Zuccarello [9], were used and the signal was normalized according to a suitable RMS value. The data is presented in Table 3.

Table 3: Material parameters [9] and RMS for the fatigue-life calculation

	$C$ [MPa $^k$ ]	$k$	$S_u$ [MPa]	RMS [MPa]
Steel	$1.934 \cdot 10^{12}$	3.324	725	5
Aluminum	$6.853 \cdot 10^{19}$	7.300	446	10
Spring steel	$1.413 \cdot 10^{37}$	11.760	1850	100

The rainflow ranges must be corrected for the cycle means with (42) before determining the relative error of the Petrucci-Zuccarello life estimate with Equation (47).

The number of cycles (and half-cycles) counted in the time history of a single random process ranged from  $1.4 \times 10^5$  to  $2.6 \times 10^5$ . The stability of fatigue-life estimate at mentioned cycle counts was checked. The relative error of an estimate for a signal fragment relative to complete (300 seconds) time-history fell below 1 % at around 100 second long time-history.

For real-life applications it is very important that the damage-estimation method does not rely on the properties of the response spectra (*e.g.*, narrow band, close modes, etc.); therefore, in this research we are trying to find the best methods in the sense that they perform well, regardless of the test group being analyzed. For the materials in Table 3, the results in Table 4, 5 and 6 show the percentage of life estimates for each method that are inside a certain margin of error, taking into account all the used spectra. For instance, for 21 % of samples the NB estimation method's relative error is less than 0.2, according to Table 4.

Table 4: Percentage of relative errors for different margins for  $k = 3.324$ 

	rel. error			
	< 0.05	< 0.1	< 0.2	< 0.5
<b>NB</b>	0	0	21	75
<b>WL</b>	18	25	62	80
<b>AL</b>	0	0	27	87
<b>GM</b>	0	0	39	100
<b>DK</b>	86	100	100	100
<b>ZB1</b>	42	91	100	100
<b>ZB2</b>	65	96	100	100
<b>TB1</b>	0	31	80	100
<b>TB2</b>	100	100	100	100
<b>PZ</b>	0	0	0	0
% of results				

Table 5: Percentage of relative errors for different margins for  $k = 7.3$ 

	rel. error			
	< 0.05	< 0.1	< 0.2	< 0.5
<b>NB</b>	0	0	0	71
<b>WL</b>	14	19	56	80
<b>AL</b>	0	0	2	75
<b>GM</b>	0	0	0	100
<b>DK</b>	15	37	83	100
<b>ZB1</b>	7	22	69	100
<b>ZB2</b>	20	25	64	100
<b>TB1</b>	0	4	33	100
<b>TB2</b>	40	71	100	100
<b>PZ</b>	7	25	25	38
% of results				

Table 6: Percentage of relative errors for different margins for  $k = 11.76$ 

	rel. error			
	< 0.05	< 0.1	< 0.2	< 0.5
<b>NB</b>	0	0	0	22
<b>WL</b>	6	18	41	87
<b>AL</b>	0	0	0	35
<b>GM</b>	0	0	0	14
<b>DK</b>	7	13	24	100
<b>ZB1</b>	0	0	12	90
<b>ZB2</b>	0	7	13	68
<b>TB1</b>	0	0	0	90
<b>TB2</b>	15	24	69	100
<b>PZ</b>	3	7	9	30
% of results				

Because they exhibited the best performance, the improved Tovo-Benasciutti (TB2), Dirlík (DK), Zhao-Baker (ZB1) and improved Zhao-Baker (ZB2) methods were selected for a detailed analysis; for each groups sample analysis see Figures 8, 9 and 10.

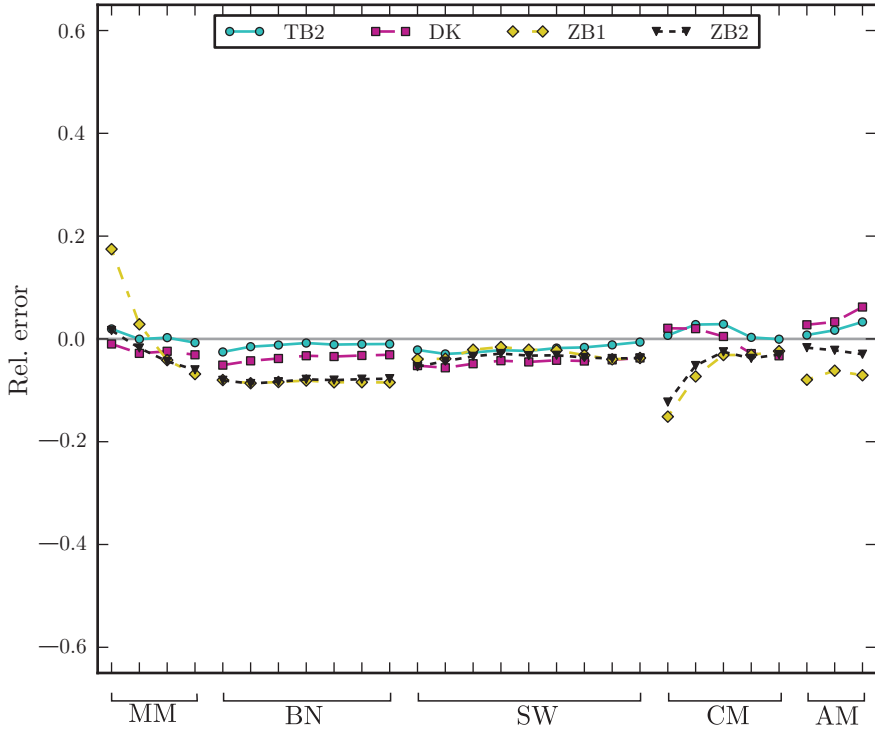


Figure 8: Comparison of the relative errors for the selected methods when  $k = 3.324$ .

## 5 Discussion

An ideal damage-estimation method for use in a design process should be consistent across different spectra and different slopes of the  $S$ - $N$  curve. It would give results that are close or equal to those given by a time-domain approach and preferably be conservative when not accurate.

Based on Tables 4, 5 and 6, a smaller number of frequency-domain methods were selected, *i.e.*, ZB1, ZB2, DK and TB2, and analyzed further. Here, a brief assessment of the accuracy for each spectral group is made and the best-performing method is chosen, based on accuracy and the consistency of the fatigue-life estimates.

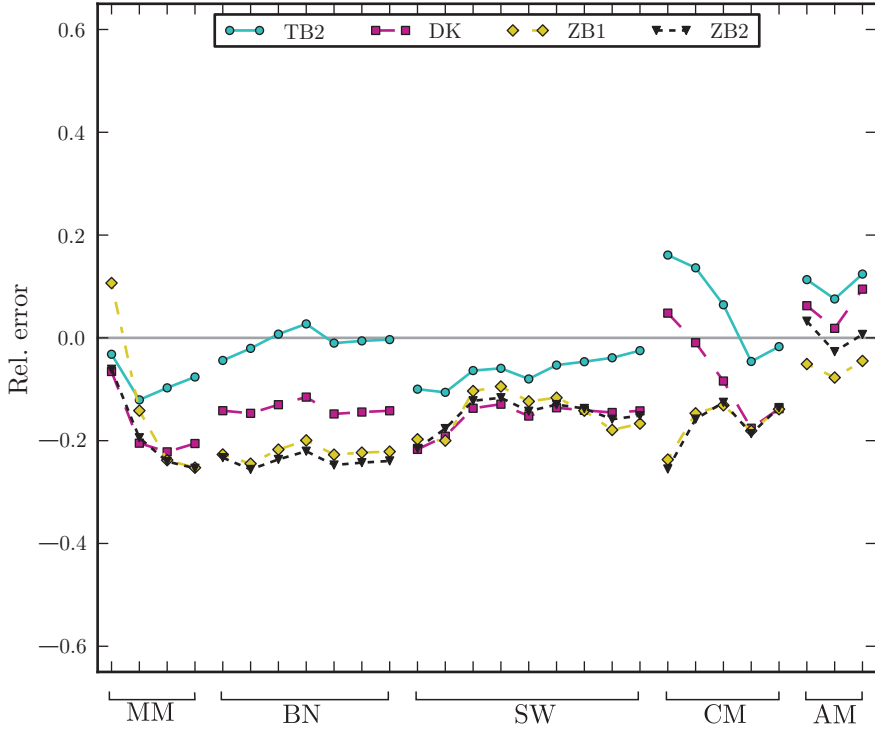


Figure 9: Comparison of the relative errors for the selected methods when  $k = 7.3$ .

### 5.1 Multi-mode

For  $k = 3.324$  the best results are obtained for the bi-modal and tri-modal spectra. For fewer modes, the chosen methods tend to overestimate the fatigue life, while for more modes they become conservative, although the relative error is still very small. The estimate is less exaggerated for higher values of  $k$  and becomes conservative at  $k = 11.76$  with all the methods. TB2 is the most accurate method in this group and manages to give a relatively close estimate, even with an  $S$ - $N$  slope of 11.760. However, only DK however, gives a conservative result for every experiment.

### 5.2 Increased background noise

The TB2 method does overestimate, in a few cases, for the BN group of spectra, but it is also much more accurate than the other three methods for all the different  $S$ - $N$  slopes  $k$ . For  $k = 3.324$  the estimates are exceptionally accurate, as is the case with all five groups of spectra. Even though DK is strictly conservative, TB2 is still the recommended method for this group, and with a much better accuracy.

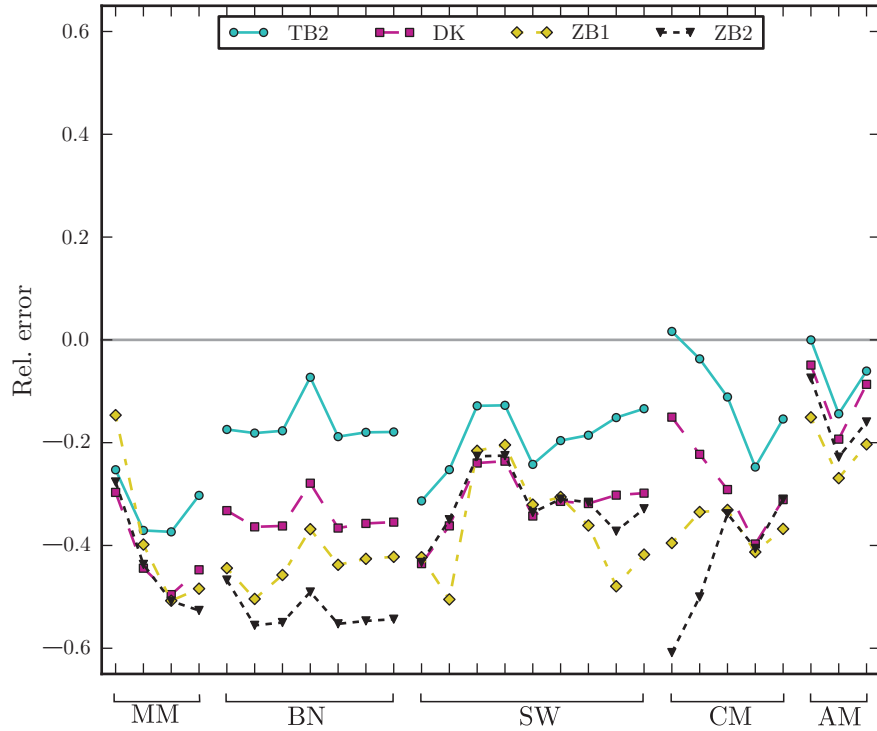


Figure 10: Comparison of the relative errors for the selected methods when  $k = 11.76$ .

### 5.3 Spectral width

Estimates for the slope  $k = 3.324$  are again very good for all four methods. However, with higher  $k$  some inconsistencies arise that affect each method. TB2 is recommended in this group because of its accurate and always-conservative estimates.

### 5.4 Close-modes

The best-performing methods overall, DK and TB2, exaggerate the fatigue life when the modes are farther apart, but with a small relative error. ZB1 and ZB2 do offer a conservative estimate at all times, but with a large relative error, especially at high values of  $k$ . It is clear that all four methods face inconsistencies with modes that are positioned far apart. TB2 is again the recommended method, but one must be aware of the overestimation problems.

## 5.5 Typical automotive spectra

The automotive spectra ZB1 and ZB2 stand out as the best-performing methods. ZB1 only slightly overestimates the fatigue life, and achieves better accuracy than ZB2, which is always conservative. Only at the highest value of the slope  $k$  do these methods fall behind DK and TB2 in terms of accuracy.

## 6 Conclusion

This theoretical and experimental research on the frequency-domain methods for vibration-fatigue estimation focuses on the questions typical for the structural dynamics (*i.e.*, close modes, noise background, mode numbers and spectral width) in the automotive accelerated test. In the theoretical background the well-established and also recent methods are presented and discussed: Dirlik, Tovo-Benasciutti (2 versions), Wirsching-Light, Zhao-Baker (2 versions), Petrucci-Zuccarello, empirical  $\alpha_{0.75}$  and the Gao-Moan method. Some of the methods have been compared with each other, while this research compares all the methods (including very recent ones) side by side. Furthermore, this research focuses on the real experimental data obtained with an electro-dynamical shaker experiment. The vibration profiles typical in structural dynamics and in an automotive-industry accelerated test are analyzed. Thus a group of best performing methods is selected, which can be applied to a general broad-band spectra. At the same time, an estimate of the error one can expect is provided.

The frequency-based methods are compared to the time-domain rainflow method. Twenty-eight different fatigue loads (5 different groups of loads) were experimentally compared. If all 28 loads are evaluated, then the improved Tovo-Benasciutti is found to be the best method, followed by the improved Zhao-Baker and Dirlik methods. These findings are in contrast to the findings of Benasciutti and Tovo [22, 13], who obtained better results with the Dirlik method.

Overall, the Dirlik, Zhao-Baker and Tovo-Benasciutti frequency-domain methods are all very consistent when the material fatigue parameter  $k$  ( $S$ - $N$  slope) is relatively low ( $k \approx 3$ ). With steeper slopes the error increases. Similar conclusions were already made by Bouyssy *et al.* [20] and Benasciutti and Tovo [22].

By analyzing selected load groups it was found that the improved Tovo-Benasciutti method gives the most accurate results if the increased background noise spectrum is increased or if the spectral width is increased. For the close-modes group and for the multi-mode group the improved Tovo-Benasciutti method was found to give a non-conservative damage estimation, while the Dirlik method always gave a conservative estimation; however, for the higher values of the material fatigue parameter  $k$  the Dirlik estimation error (compared to the rainflow time-domain method) is up to 50%. The improved Zhao-Baker method was found to be the most accurate (giving a conservative fatigue-damage estimation) for the typical automotive-industry accelerated test profiles.

This research showed that the improved Tovo-Benasciutti and the improved Zhao-Baker methods should also be considered together with the Dirlik method. In general, the improved Tovo-Benasciutti method gives best results, while the improved Zhao-Baker method gives the best results for the tested vibration profiles typical in the automotive industry.

## References

- [1] I. Rychlik. Fatigue and stochastic loads. *Scand. J. Stat.*, 23(4):387–404, 1996.
- [2] M. Matsuishi and T. Endo. Fatigue of metals subject to varying stress. *Paper presented to Japan Society of Mechanical Engineers, Fukuoka, Japan*, 1968.
- [3] A. Palmgren. Die lebensdauer von kugellagern. *VDI-Zeitschrift*, 68:339–341, 1924.
- [4] MA Miner. Cumulative damage in fatigue. *J. Appl. Mech.*, 12:A159–A164, 1945.
- [5] G Petrucci and B Zuccarello. On the estimation of the fatigue cycle distribution from spectral density data. *Proceedings of the institution of mechanical engineers part C - J. Eng. Sci.*, 213(8):819–831, 1999.
- [6] A Halfpenny. A frequency domain approach for fatigue life estimation from finite element analysis. In M. D. Gilchrist, J. M. DulieuBarton, and K. Worden, editors, *DAMAS 99: Damage Assessment of Structures*, volume 167-1 of *Key Engineering Materials*, pages 401–410, 1999.
- [7] W. Zhao and M. J. Baker. On the probability density function of rainflow stress range for stationary gaussian processes. *Int. J. Fatigue*, 14(2):121–135, March 1992.
- [8] R. Tovo. Cycle distribution and fatigue damage under broad-band random loading. *Int. J. Fatigue*, 24(11):1137–1147, 2002.
- [9] G. Petrucci and B. Zuccarello. Fatigue life prediction under wide band random loading. *Fatigue & Fract. Eng. Mater. & Struct.*, 27(12):1183–1195, December 2004.
- [10] K. Shin and J. K. Hammond. *Fundamentals of signal processing for sound and vibration engineers*. John Wiley & Sons, Ltd, 2008.
- [11] L. D. Lutes and S. Sarkani. *Random vibrations: analysis of structural and mechanical systems*. Elsevier, 2004.
- [12] T. Dirlik. *Application of Computers in Fatigue Analysis*. PhD thesis, The University of Warwick, 1985.

- [13] D. Benasciutti and R. Tovo. Spectral methods for lifetime prediction under wide-band stationary random processes. *Int. J. Fatigue*, 27(8):867–877, 2005.
- [14] N. W. M. Bishop. *The use of frequency domain parameters to predict structural fatigue*. PhD thesis, University of Warwick, 1988.
- [15] Costas Papadimitriou, Claus-Peter Fritzen, Peter Kraemer, and Evangelos Ntotsios. Fatigue predictions in entire body of metallic structures from a limited number of vibration sensors using kalman filtering. *Struct. Control Health Monit.*, 18(5):554–573, 2011.
- [16] J. Slavič, T. Opara, R. Banov, M. Dogan, M. Česnik, and M. Boltežar. Development of next-generation vibration-fatigue software and catia integration for the automotive industry. pages 117–125. Belgrade: Yugoslav Society of Automotive Engineers, 2011.
- [17] A. Cristofori, D. Benasciutti, and R. Tovo. A stress invariant based spectral method to estimate fatigue life under multiaxial random loading. *Int. J. Fatigue*, 33(7):887–899, 2011.
- [18] C. Braccesi, F. Cianetti, G. Lori, and D. Pioli. The frequency domain approach in virtual fatigue estimation of non-linear systems: The problem of non-gaussian states of stress. *Int. J. Fatigue*, 31(4):766–775, 2009.
- [19] N. W. M. Bishop, Z. Hu, R. Wang, and D. Quarton. Methods of rapid evaluation of fatigue damage on howden HWP330 wind turbine. 1993.
- [20] V. Bouyssy, S. M. Nabobikhov, and R. Rackwitz. Comparison of analytical counting methods for gaussian processes. *Struct. Saf.*, 12(1):35–57, 1993.
- [21] Z. Ghao and T. Moan. Frequency-domain fatigue analysis of wide-band stationary gaussian processes using a trimodal spectral formulation. *Int. J. Fatigue*, 30(10-11):1944–1955, 2008.
- [22] D. Benasciutti. *Fatigue analysis of random loadings*. PhD thesis, University of Ferrara, Italy, 2004.
- [23] P. H. Wirsching and M. C. Light. Fatigue under wide band random stresses. *J. Struct. Div. ASCE*, 106(7):1593–1607, 1980.
- [24] T Lagoda, E Macha, and A Nieslony. Fatigue life calculation by means of the cycle counting and spectral methods under multiaxial random loading. *Fatigue & Fract. Eng. Mater. & Struct.*, 28(4):409–420, April 2005.
- [25] C Braccesi, F Cianetti, G Lori, and D Pioli. Fatigue behaviour analysis of mechanical components subject to random bimodal stress process: frequency domain approach. *Int. J. Fatigue*, 27(4):335–345, April 2005.
- [26] T. Fu and D. Cebon. Predicting fatigue lives for bimodal stress spectral densities. *Int. J. Fatigue*, 22(1):11–21, January 2000.

- [27] S. Sakai and H. Okamura. On the distribution of rainflow range for gaussian random loading processes with bimodal psd. *JSME Int. J.*, 38(4):440–445, October 1995.
- [28] J. Bendat. Probability functions for random responses. In *NASA report*. 1964.
- [29] Y. M. Low. A method for accurate estimation of the fatigue damage induced by bimodal processes. *Probab. Eng. Mech.*, 25(1):75–85, January 2010.
- [30] T. Lagoda, E. Macha, and A. Nieslony. Comparison of the rain flow algorithm and the spectral method for fatigue life determination under uniaxial and multiaxial random loading (conference paper). In *ASTM Special Technical Publication*, number 1439, pages 544–556, 2003, Fatigue Testing and Analysis Under Variable Amplitude Loading Conditions.
- [31] C. J. Kim, Y. J. Kang, and B. H. Lee. Experimental spectral damage prediction of a linear elastic system using acceleration response. *Mech. Syst. Signal Process.*, 25(7):2538–2548, October 2011.
- [32] M. Čermelj and M. Boltežar. Modelling localised nonlinearities using the harmonic nonlinear super model. *J. Sound Vib.*, 298(4-5):1099–1112, 2006.
- [33] D. E. Newland. *An introduction to Random vibrations and spectral analysis*. Longman Scientific & Technical, 1993.
- [34] E. H. Vanmarcke. Properties of spectral moments with applications to random vibration. *J. Eng. Mech. Div. ASCE*, 98:425–446, 1972.
- [35] S. O. Rice. Mathematical analysis of random noise. *Bell Syst. Tech. J.*, 23(3), 1944.
- [36] N. W. M. Bishop and F. Sherratt. *Finite Element Based Fatigue Calculations*. NAFEMS Ltd, October 2000.
- [37] N. M. M. Maia and J. M. M. Silva. *Theoretical and Experimental Modal Analysis*. Research Studies Pre, 1997.
- [38] J. W. Miles. On structural fatigue under random loading. *J. Aeronaut. Soc.*, 21:753–762, 1965.
- [39] A. Zalaznik and M. Nagode. Frequency based fatigue analysis and temperature effect. *Mater. & Des.*, 32(10):4794–4802, December 2011.
- [40] J. Goodman. *Mechanics applied to engineering*. Longman, Green & Co., 1954.